https://doi.org/10.32056/KOMAG2025.16

# Analysis of water flow through a nozzle taking into account heat transfer using CFD numerical modeling

Received: 30.10.2025 Accepted: 05.11.2025

Published online: 14.11.2025

#### Author's affiliations and addresses:

<sup>1</sup> SUPERSNOW S.A. Ks. Antoniego Siudy 11 34-436 Maniowy, Poland

 <sup>2</sup> AGH University of Science and Technology in Krakow
Al. Adama Mickiewicza 30

30-059 Krakow, Poland

# ${\bf * Correspondence:}$

e-mail: rokitom@agh.edu.p

Robert MOCZARNY <sup>1</sup>, Dariusz KACZOR<sup>1</sup>, Tomasz ROKITA<sup>1</sup><sup>2\*</sup>

#### Abstract:

This article presents the results of numerical flow simulations, taking into account heat transfer in water nozzle components. Analyses were conducted using computer simulations, including the finite volume method in Siemens FLOEFD for NX. A free surface function was used to ensure free water flow through the nozzle outlet. Flow simulations were performed for four calculation cases. Identical air parameters outside the nozzle were assumed for all calculation cases. The first two calculation cases, for pressures of 15 bar and 40 bar, respectively, considered the swirler and atomizer material as MO58, while the next two, also for pressures of 15 bar and 40 bar, considered the nozzle components as Al<sub>2</sub>O<sub>3</sub> – 98%. The volumetric flow rate of water through the nozzle was determined to be 3.7 l/min for pressures of 15 bar and 6 l/min for pressures of 40 bar. For each flow simulation, maps of the temperature, pressure, and velocity distribution of the water and air flowing through the nozzle were presented. Additionally, for each simulation, the temperature distribution on the outer surface of the nozzle, within the outlet opening and in the YZ cross-section was presented.

Keywords: water nozzle, numerical flow calculations, CFD analysis, finite volume method, thermal analysis

#### 1. Introduction

The growing interest in winter physical activity in mountainous regions requires snowmakers to be more efficient, especially at temperatures above 0°C. The basic design element of a snowmaker is the water nozzle, which is manufactured based on a combination of theoretical formulas, laboratory tests, numerical modelling, and industrial verification. The nozzle geometry directly affects the efficiency of the jets, which are then used for subsequent applications such as spraying, cleaning, cutting, and drilling [1, 2, 3]. Due to the time-consuming process of preparation and laboratory testing, the fluid mechanics and heat transfer analysis of the designed water nozzle is performed using numerical modelling. Li et al. [4] performed three-dimensional numerical simulations of round-rectangular nozzles using Fluent 6.0 CFD software with user-defined functionality. Based on their studies, they found that the outlet height-to-width ratio has a significant impact on flow and heat transfer in roundrectangular nozzles. Too small a ratio disrupts the flow field in the nozzles and leads to high temperature points and even nozzle burnout. Reis and dos Santos Gioria [5] conducted a CFD study of the nozzle diameter, nozzle outlet position, mixing length, diffuser curve, and diameter in a waterwater ejector. Kuś and Madejski [6] developed an axisymmetric CFD model of an ejector condenser to investigate the ejector efficiency and condensation intensity for different design modes. In their research, they used Simcenter STAR-CCM+ software based on the finite volume method. Buska et al. [7] used Ansys Fluent Meshing software and the Poly-Hexcore Mosaic mesh to investigate water nozzles of varying shapes and their effects on water jet flow, concentration, dispersion, and range. Regarding nozzle structure, Wen and Chen [8] investigated the jet characteristics of nozzles with different structures using a simple conical nozzle model. Jiang et al., [9] numerically studied the discharge field of various nozzles with different inlet velocities and different convergence angles. They found that a nozzle with a convergence angle of 10 or 15° and three times the outlet diameter was characterized by a longer flow core, better agglomeration efficiency, and a higher discharge coefficient. Pan et al. [10] used Fluent software, in which the k-ɛ turbulence model was used to simulate the flow of nozzles with different sizes and nozzle arrangements in the pipeline. Martínez and Gaukel [11] modelled pneumatic atomizers using experimental data collected for different air pressures and feed fluid viscosities.

#### 2. Finite volume method

The finite volume method (FVM) is a numerical method for solving partial differential equations. The method is based on representing the differential equation as a system of algebraic equations. The search values are computed at nodes. This method uses a mesh that approximates the shape of the object. A control region is constructed around a given node [12]. In this region, a condition described by a differential equation is required. This condition need not be satisfied for the entire volume of the object. The control region is equivalent to a grid mesh or is constructed independently of it. The discussed method uses the Gauss-Ostrogradsky theorem to convert a volume integral into a surface integral. This theory states that the output flux of a vector field passing through a closed surface is equal to the volume integral of the divergence of this vector field in the volume enclosed by the surface [13]. This method is commonly used in fluid mechanics.

In this article, geometric models were prepared in ANSYS Discovery SpaceClaim software. The numerical model for flow calculations was built using the Siemens FLOEFD tool for NX. The results were also presented in the Siemens FLOEFD software. The aforementioned Siemens FLOEFD numerical software enables, among other things, thermal analyses and CFD flow analyses using the finite volume method described above. The numerical analyses presented in the article included simulation of water flow through a water nozzle and analysis of heat transfer through nozzle elements, taking into account the flow of air.

## 3. Numerical modeling

## 3.1. Nozzle geometry and material

The subject of the modeling was a water nozzle (Figure 1) consisting of the following elements: a 2020 version IV water nozzle nut - 2 mm holder, a flexible nozzle expansion holder, a nozzle swirler mounting washer, a 2020 swirler -  $3x30stx1.5x1.5 + \phi1x1$  hole, and a nozzle sprayer. The surface roughness was assumed to be Ra 3.2.

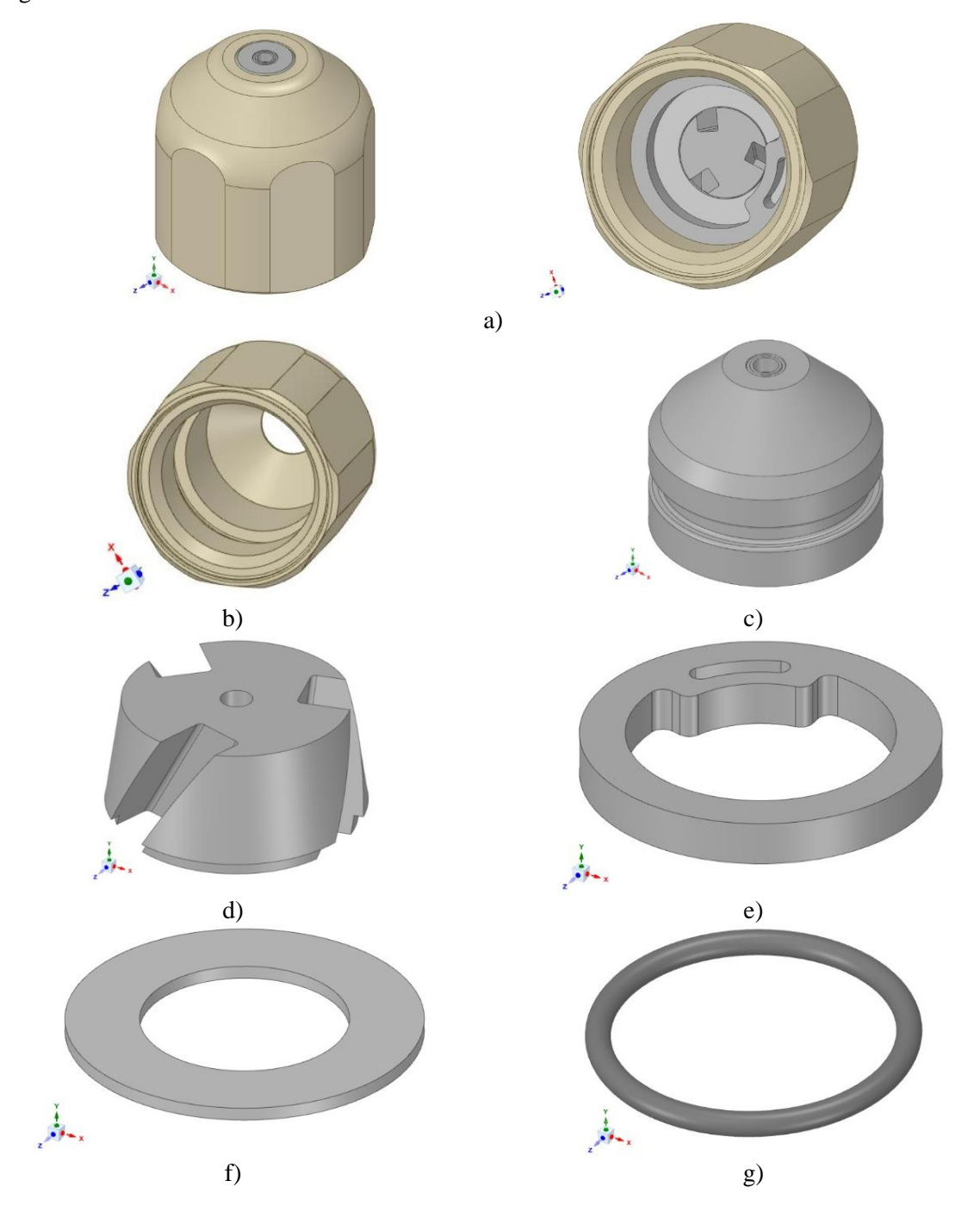


**Fig. 1.** Nozzle components: a) 3D view; b) nut; c) nozzle; d) swirl element; e) flexible expansion holder; f) mounting washer; g) seal

For the numerical analysis, it was assumed that the nozzle material would be manufactured in two variants (Table 1). Table 2 presents the material data for all materials defined in the numerical analyses [14, 15]. All materials are considered homogeneous throughout.

Analysis I Swirler 2020 - 3x30mm x 1.5 mm x Nozzle sprayer 2020 + cutting edge Water nozzle nut 2020 version IV Flexible nozzle expansion holder Nozzle swirler mounting washer 1.5 mm, 5 mm + 1 mm hole PN-M- 73093 11x1 (PN-M) SUPERSNOW 202 2 mm holder 2020 version Item name **Brass MO58** (according to PN) Stainless **Brass** Material Rubber **Brass MO58 EPDM** electrochemically steel 1.4401 **MO58** nickel-plated Analysis II **Brass MO58** Aluminum Aluminum (according to PN) Stainless oxide Material Rubber oxide Al<sub>2</sub>O<sub>3</sub> **EPDM** electrochemically steel 1.4401  $Al_2O_3$  -- 98% nickel-plated 98%

**Table 1.** Nozzle component materials for analysis

Table 2. Material data

Material	Density [kg/m³]	Specific heat [J/(kg*K)]	Thermal conductivity coefficient [W/(m*K)]
Al <sub>2</sub> O <sub>3</sub> 98%	3817	880	30.59
MO58	8430	0.377	113
1.4401	8000	500	15
Rubber	1200	1000	0.15

The physical properties of alumina  $Al_2O_3$  - 98% were calculated based on the values from the material certificate for  $Al_2O_3$  - 94%,  $Al_2O_3$  - 96%,  $Al_2O_3$  - 99.5% provided by SUPERSNOW [16].

### 3.2. Computational model

The computational model consisted of a geometric model (Figure 2a) and a numerical (discrete) model (Figure 2b) built for CFD flow and thermal analyses. The discrete models were built based on the geometric models. Figures 3a-3f present the discrete models used in the numerical analyses.



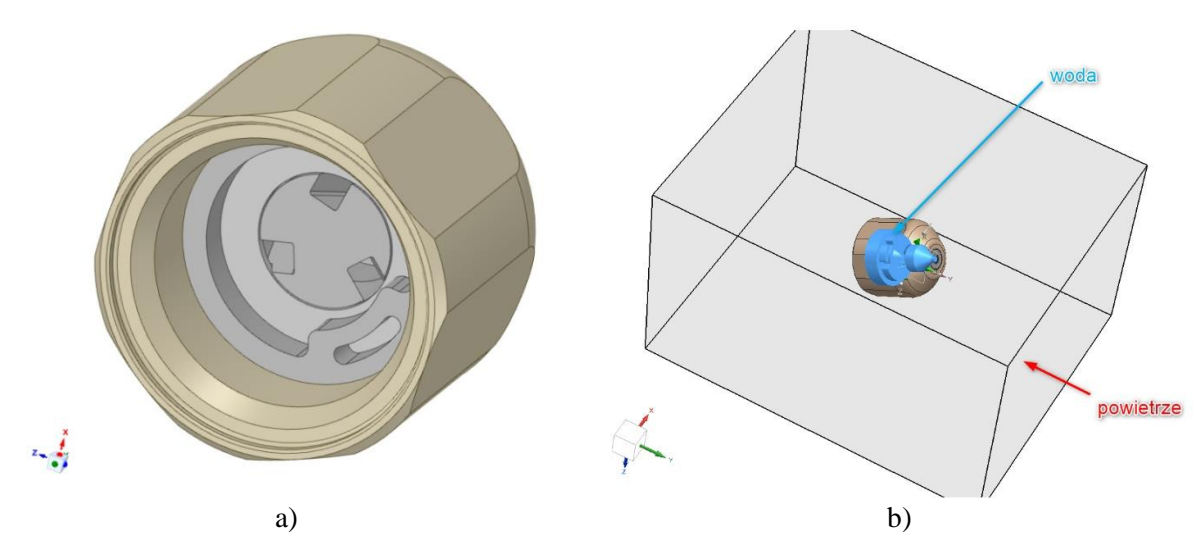
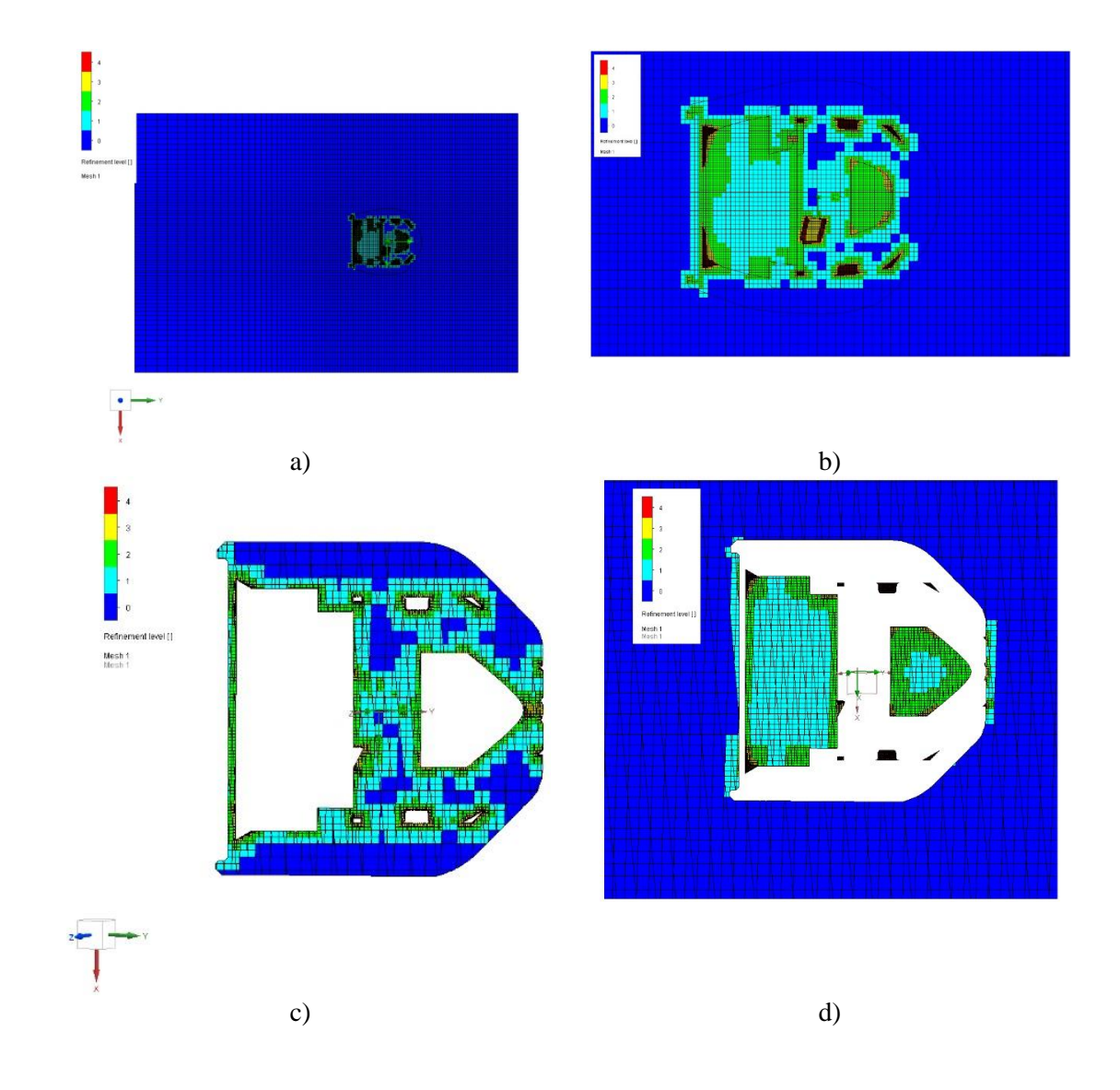
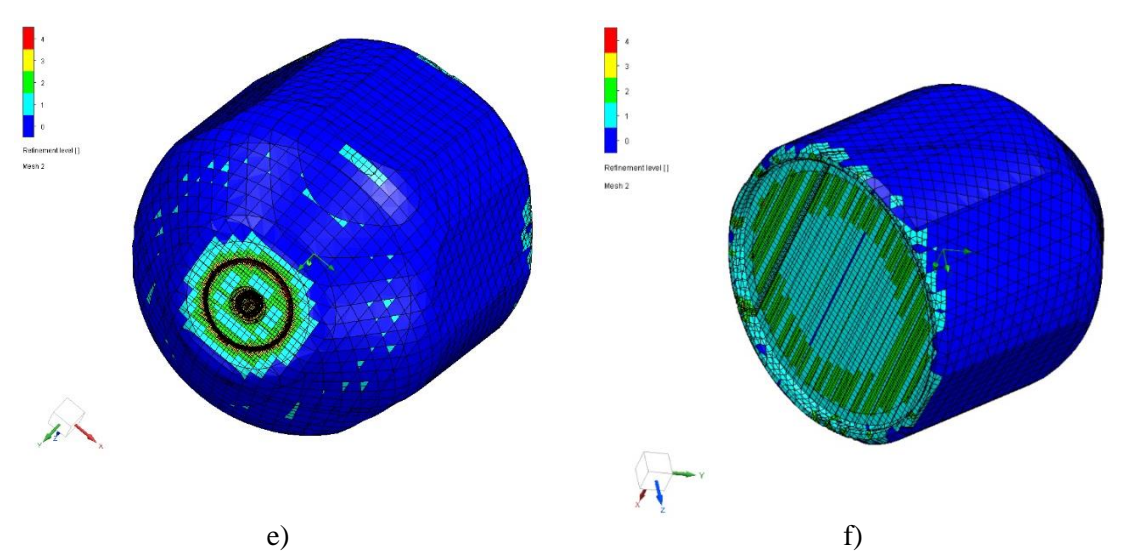


Fig. 2. Computational model: a) geometric; b) numerical





**Fig. 3.** Discrete model: a) computational domain - cross-section 1; b) computational domain - cross-section 2; c) Solid elements - cross-section 3; d) Fluid elements - cross-section 4; e) visualization of the computational mesh on the surface of nozzle 1; f) visualization of the computational mesh on the surface of nozzle 2

#### 3.3. Boundary conditions

For all analyses, the water temperature inside the nozzle is 0.3°C, while the air temperature flowing through the nozzle is -20°C. The air velocity in the Y direction is 40 m/s for all analyses. The axis of the water nozzle outlet is directed at a 30° angle to the air flow direction vector (Figure 4).

For each analysis (I and II), calculations were performed for two design cases: a pressure of 15 bar (Figure 5) and a pressure of 40 bar at the nozzle inlet (Figure 6). The analyses were performed for the same boundary conditions. Only the material data changed. All material data, depending on the analysis, were assumed in accordance with the information presented in Tables 1 and 2.

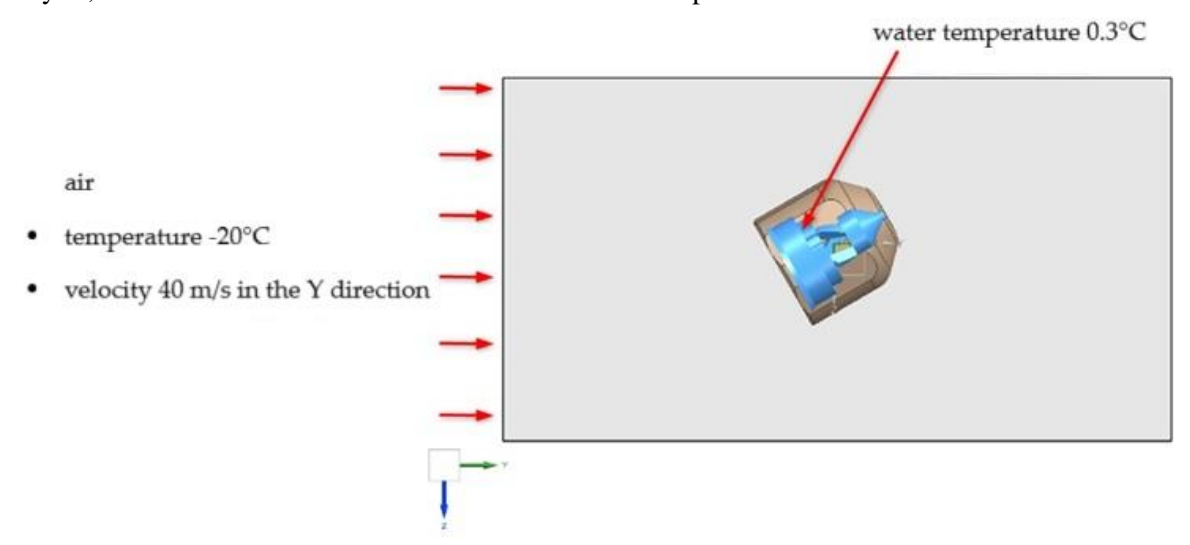


**Fig. 4.** Temperature and velocity values for all analyses performed, water temperature 0.3°C

The pressure set at the nozzle inlet for the first calculation case is 15 bar. Analyses were performed using the free surface function. The pressure outside the nozzle was set to 1 atm for the air medium. The medium conditions were set as shown in Figure 5.

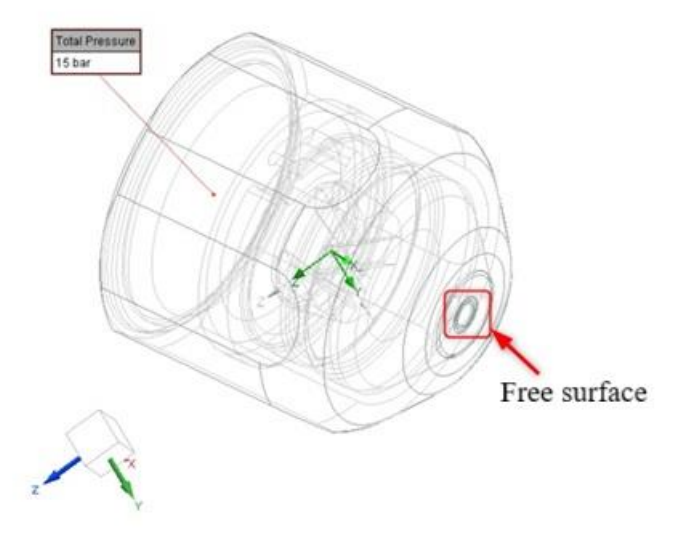


Fig. 5. Boundary conditions – inlet pressure 15 bar, free surface at the nozzle outlet

The pressure set at the nozzle inlet for the second design case is 40 bar. The pressure set at the outlet is 1 atm. The medium conditions are set as shown in Figure 6.

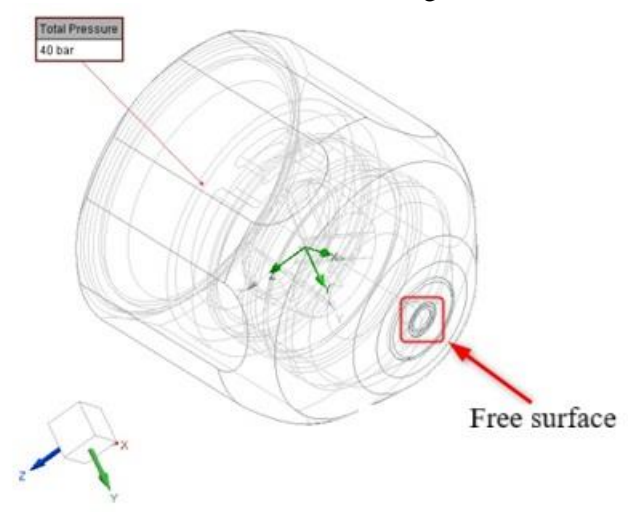


Fig. 6. Boundary conditions – inlet pressure 40 bar, free surface at the nozzle outlet

# 4. CFD modeling results

CFD flow simulation results, taking into account heat transfer in nozzle components, were performed for four simulations: Analysis I, including nozzle components (swirler and nozzle atomizer) made of MO58 brass:

- nozzle inlet pressure: 15 bar,
- nozzle inlet pressure: 40 bar.

Analysis II, including nozzle components (swirler and nozzle atomizer) made of  $98\%~Al_2O_3$  alumina:

- nozzle inlet pressure: 15 bar,
- nozzle inlet pressure: 40 bar.



The input parameters for Analysis I and II are presented in Tables 3 and 4.

Parameter	Pressure 15 bar	Pressure 40 bar
Water temperature	0.3°C	0.3°C
Nozzle inlet pressure	15 bar	40 bar
Water density	1000.54 kg/m <sup>3</sup>	1001.79 kg/m <sup>3</sup>
Temperature of the air flowing through the nozzle	-20°C	-20°C
The velocity of the air flowing through the nozzle	40 m/s	40 m/s
Swirler and atomizer material	MO58	MO58

Table 4. Input parameters for analysis II

Parameter	Pressure 15 bar	Pressure 40 bar
Water temperature	0.3°C	0.3°C
Nozzle inlet pressure	15 bar	40 bar
Water density	1000.54 kg/m <sup>3</sup>	1001.79 kg/m <sup>3</sup>
Temperature of the air flowing through the nozzle	-20°C	-20°C
The velocity of the air flowing through the nozzle	40 m/s	40 m/s
Swirler and atomizer material	Al <sub>2</sub> O <sub>3</sub> - 98%	Al <sub>2</sub> O <sub>3</sub> - 98%

The air flow conditions around the nozzle are the same for all simulations, therefore the air flow distribution is presented only for the first simulation, but it applies to all presented analyses (Figure 7).

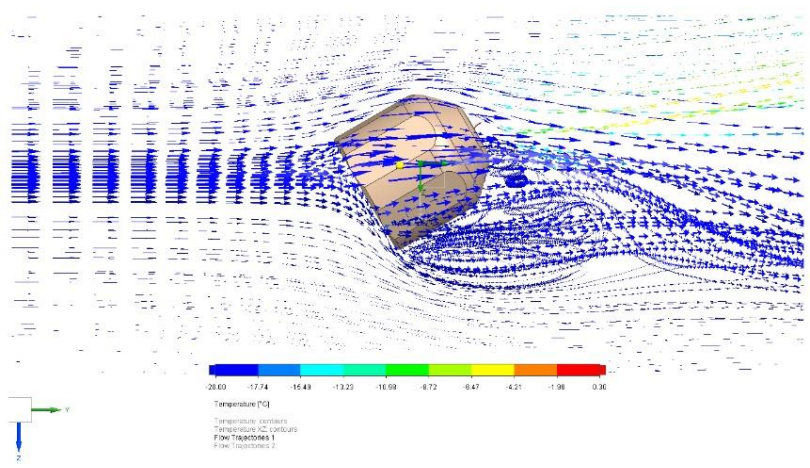


Fig. 7. Distribution of the air flow around the nozzle

Figures 8-17 present the results for two materials: MO58 and Al<sub>2</sub>O<sub>3</sub>, at pressures of 15 bar and 40 bar, in particular:

- nozzle volumetric efficiency for a given pressure - Figures 8a-8d;



- medium pressure distribution on a scale of 1-15 bar and 0-40 bar Figures 9a-9d;
- medium pressure distribution cross-section along the swirl groove axis Figures 10a-10d;
- velocity distribution YZ cross-section view of the nozzle Figures 11a-11d, 12a-12d (enlarged);
- velocity distribution cross-section along the swirl groove axis Figures 13a-13d;
- medium temperature distribution from -20°C to 0.3°C YZ cross-section view of the nozzle Figures 14a-14d;
- temperature distribution on the surface at the nozzle outlet Figure 15a-15d;
- temperature distribution on the nozzle nut surface Figure 16a-16d;
- temperature distribution of solid elements YZ cross-section view of the nozzle Figure 17a-17d.

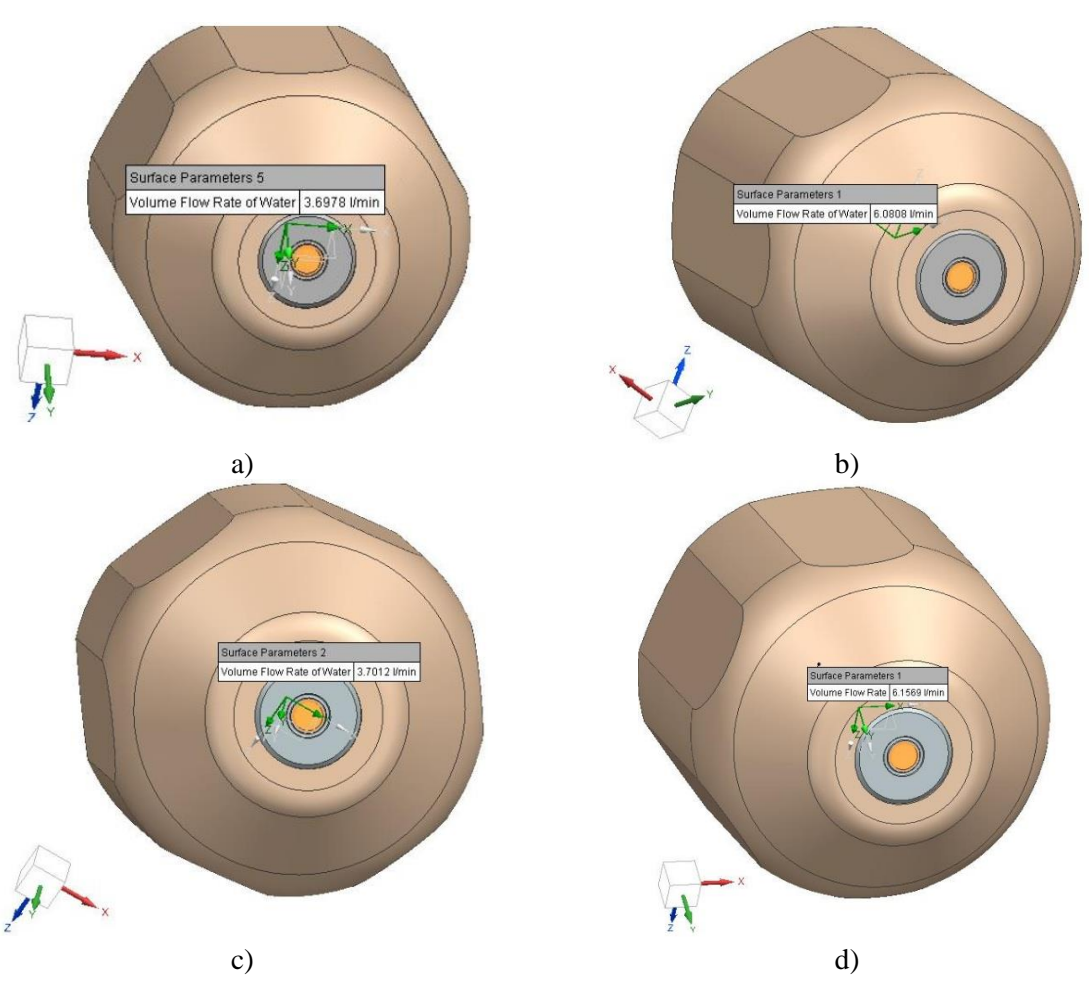


**Fig. 8.** Nozzle volumetric efficiency for pressure: a) 15 bar (analysis I); b) 40 bar (analysis I); c) 15 bar (analysis II); d) 40 bar (analysis II)

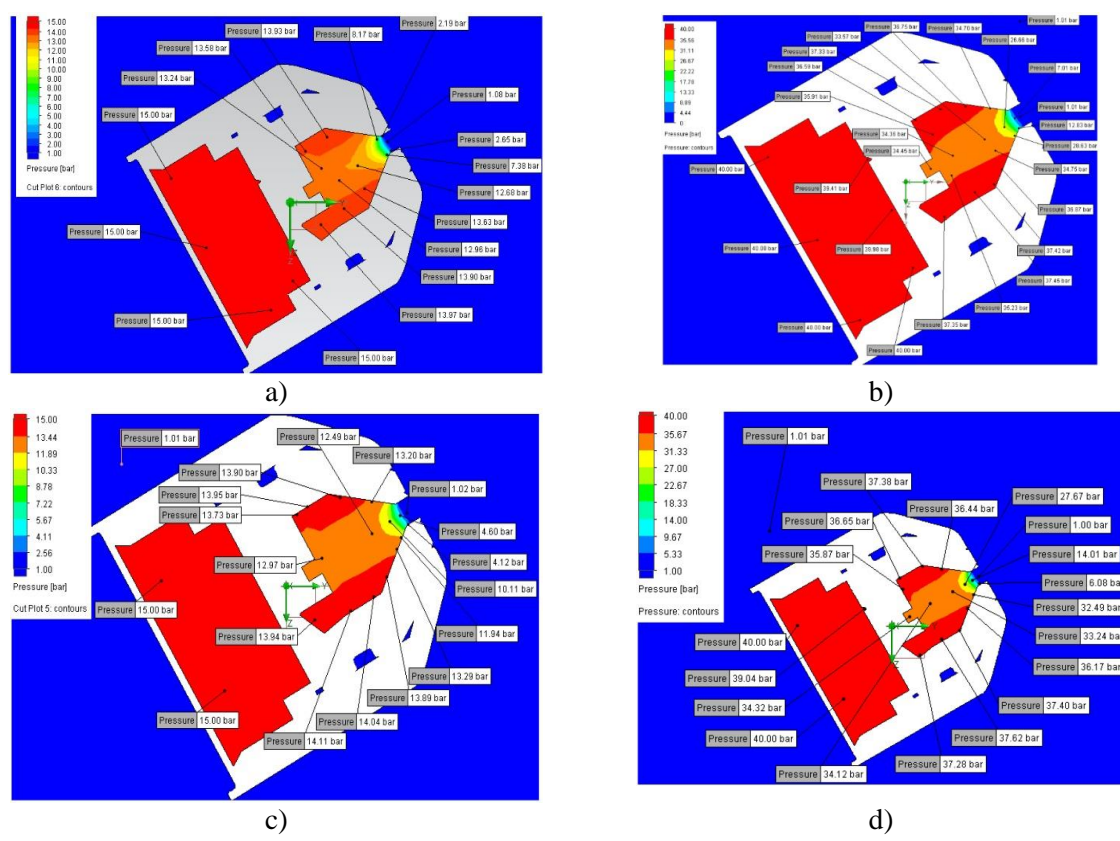


**Fig. 9.** Pressure distribution of the medium on a scale: a) 1-15 bar, swirler and atomizer material: MO58 (analysis I); b) 0-40 bar, swirler and atomizer material: MO58 (analysis I); c) 1-15 bar, swirler and atomizer material: Al<sub>2</sub>O<sub>3</sub> – 98% (analysis II); d) 1-40 bar, swirler and atomizer material: Al<sub>2</sub>O<sub>3</sub> – 98% (analysis II)

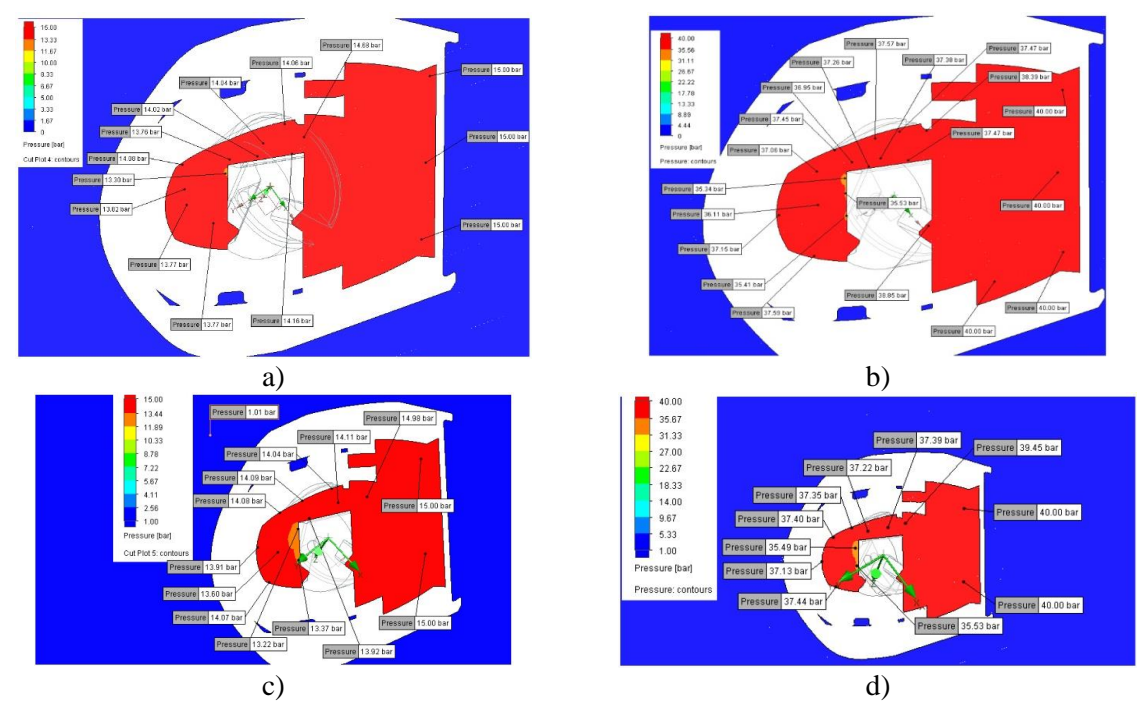


**Fig. 10.** Pressure distribution of the medium – cross-section in the axis of the swirler groove: a) swirler and atomizer material: MO58 (analysis I) 15 bar; b) MO58 (analysis I) 40 bar; c) swirler and atomizer material:  $Al_2O_3 - 98\%$  (analysis II) 15 bar; d) swirler and atomizer material:  $Al_2O_3 - 98\%$  (analysis II) 40 bar

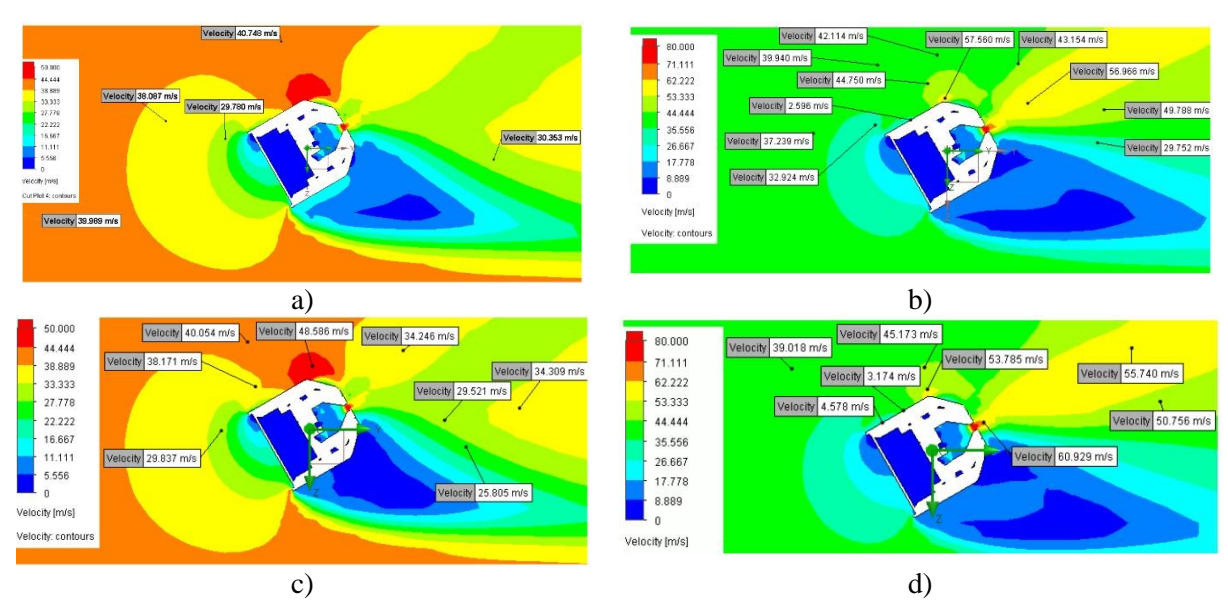


**Fig. 11.** Velocity distribution – YZ cross-section view of the nozzle: a) on a scale of 0-50 m/s, swirler and sprayer material: MO58 (analysis I) 15 bar; b) on a scale of 0-80 m/s swirler and sprayer material: MO58 (analysis I) 40 bar; c) on a scale of 0-50 m/s swirler and sprayer material: Al<sub>2</sub>O<sub>3</sub> – 98% (analysis II) 15 bar; d) on a scale of 0-80 m/s swirler and sprayer material: Al<sub>2</sub>O<sub>3</sub> – 98% (analysis II) 40 bar

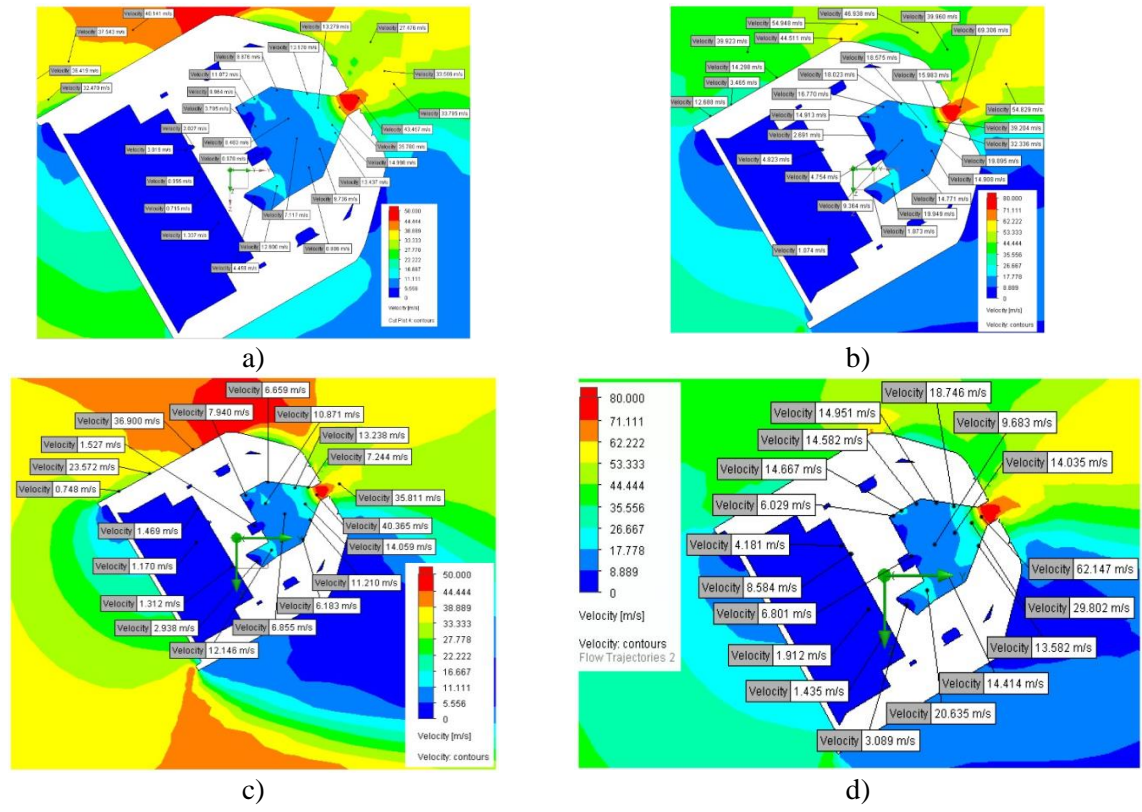


**Fig. 12.** Velocity distribution – YZ cross-section view of the nozzle (enlarged): a) on a scale of 0-50 m/s, swirler and sprayer material: MO58 (analysis I) 15 bar; b) on a scale of 0-80 m/s swirler and sprayer material: MO58 (analysis I) 40 bar; c) on a scale of 0-50 m/s swirler and sprayer material: Al<sub>2</sub>O<sub>3</sub> – 98% (analysis II) 15 bar; d) on a scale of 0-80 m/s swirler and sprayer material: Al<sub>2</sub>O<sub>3</sub> – 98% (analysis II) 40 bar

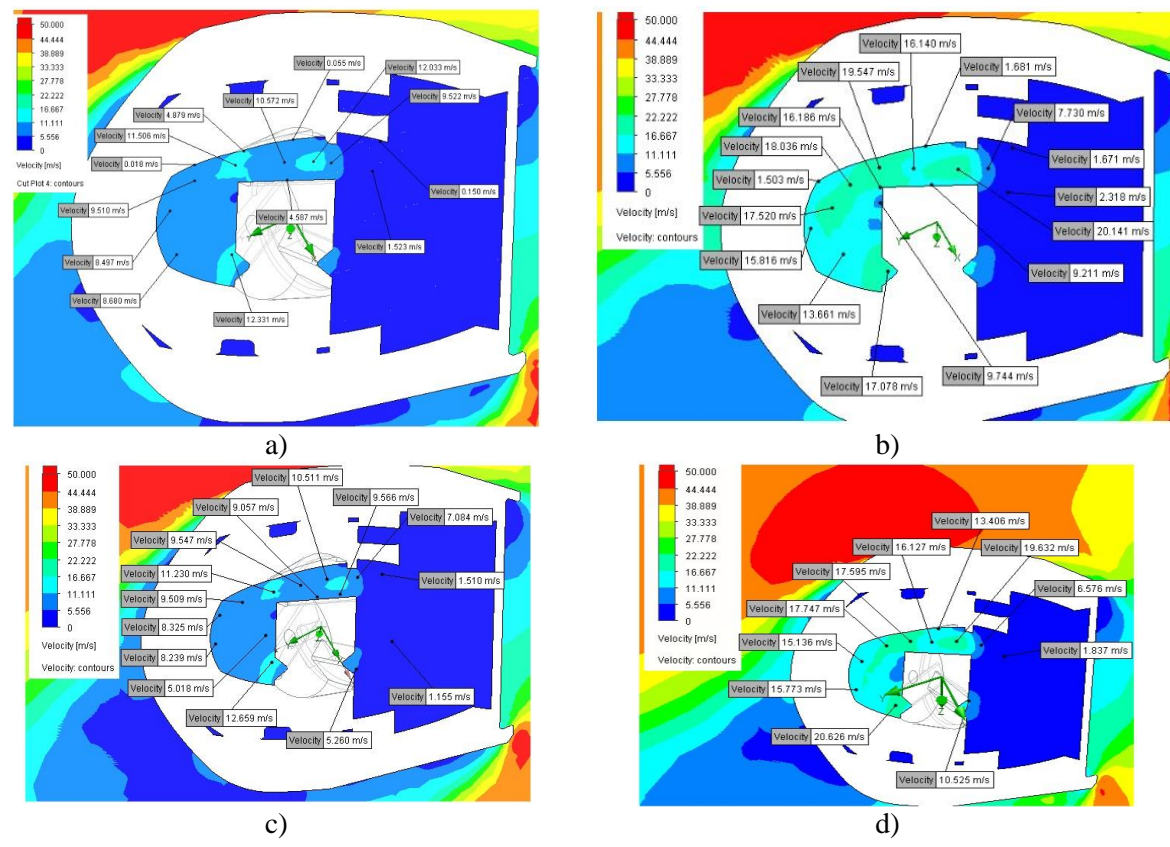


**Fig. 13.** Velocity distribution – cross-section in the swirler groove axis: a) in a scale of 0-50 m/s, p = 15 bar, swirler and atomizer material: MO58; b) p = 40 bar, swirler and atomizer material: MO58; c) swirler and atomizer material:  $Al_2O_3 - 98\%$ , d) p = 40 bar, swirler and atomizer material:  $Al_2O_3 - 98\%$ 

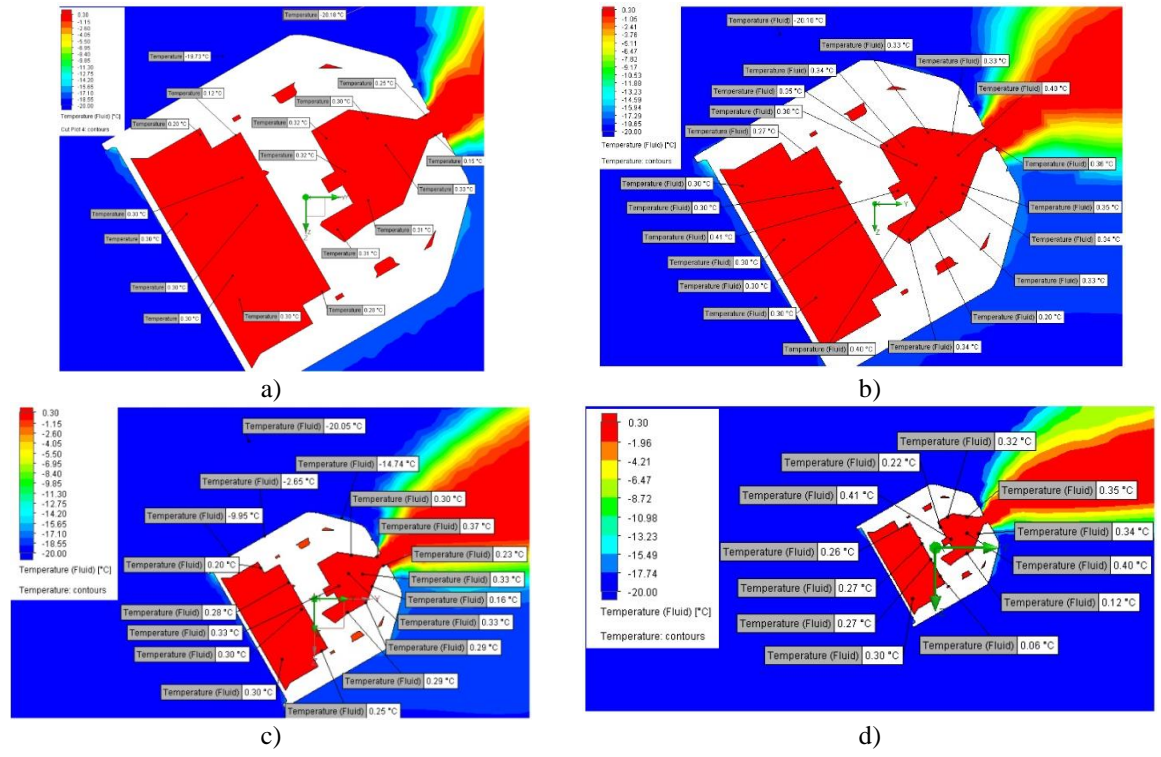


**Fig. 14.** Medium temperature distribution from -20°C to 0.3°C - YZ cross-section view of the nozzle: a) p = 15 bar, swirler and atomizer material: MO58; b) p = 40 bar, swirler and atomizer material: MO58; c) swirler and atomizer material:  $Al_2O_3 - 98\%$ , d) p = 40 bar, swirler and atomizer material:  $Al_2O_3 - 98\%$ 

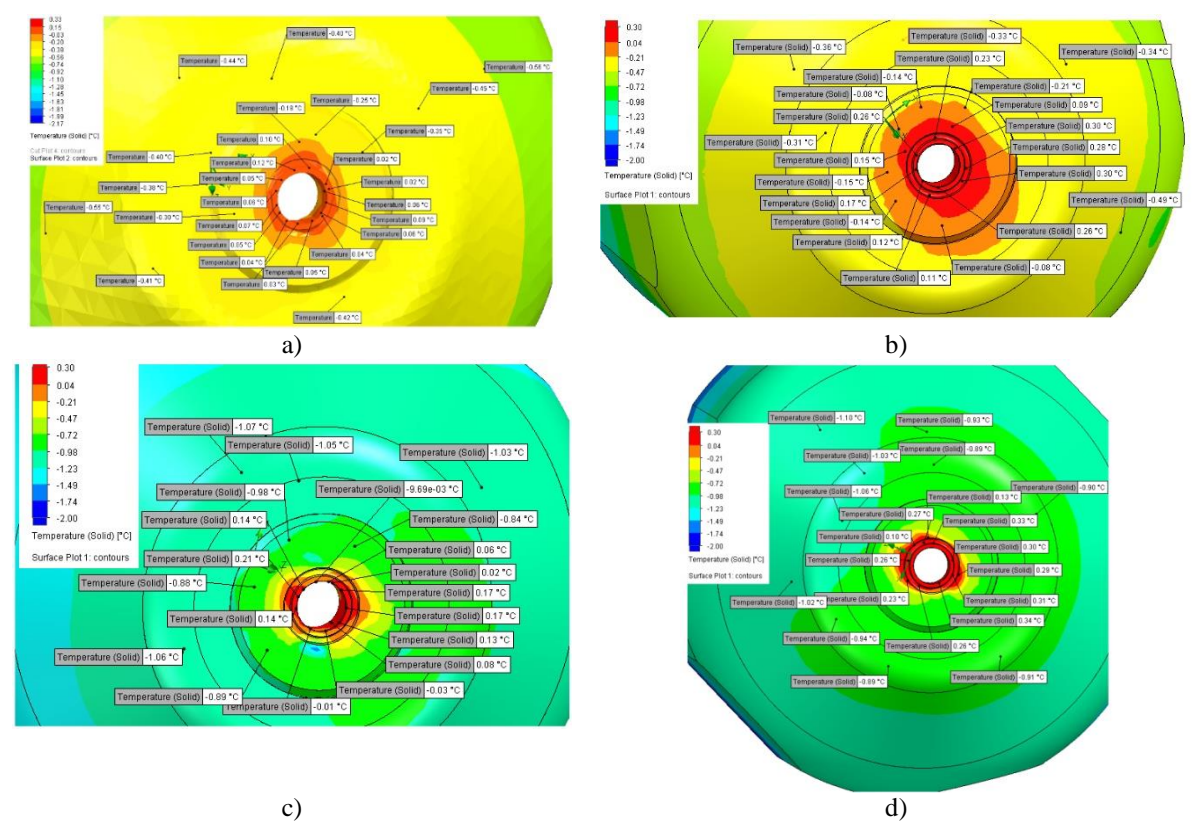


**Fig. 15.** Temperature distribution on the surface at the nozzle outlet: a) p = 15 bar, swirler and atomizer material: MO58; b) p = 40 bar, swirler and atomizer material: MO58; c) swirler and atomizer material:  $Al_2O_3 - 98\%$ ; d) p = 40 bar, swirler and atomizer material:  $Al_2O_3 - 98\%$ 

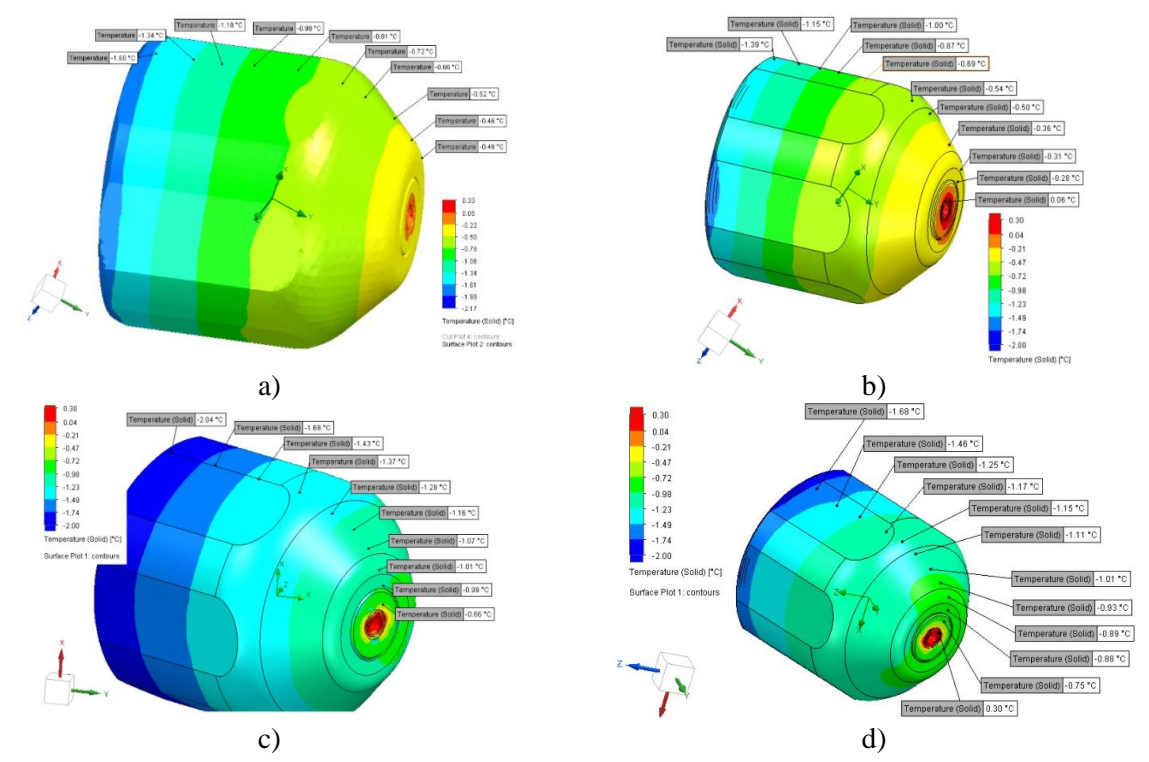


**Fig. 16.** Temperature distribution on the nozzle nut surface: a) p = 15 bar, swirler and atomizer material: MO58; b) p = 40 bar, swirler and atomizer material: MO58; c) swirler and atomizer material:  $Al_2O_3 - 98\%$ ; d) p = 40 bar, swirler and atomizer material:  $Al_2O_3 - 98\%$ 

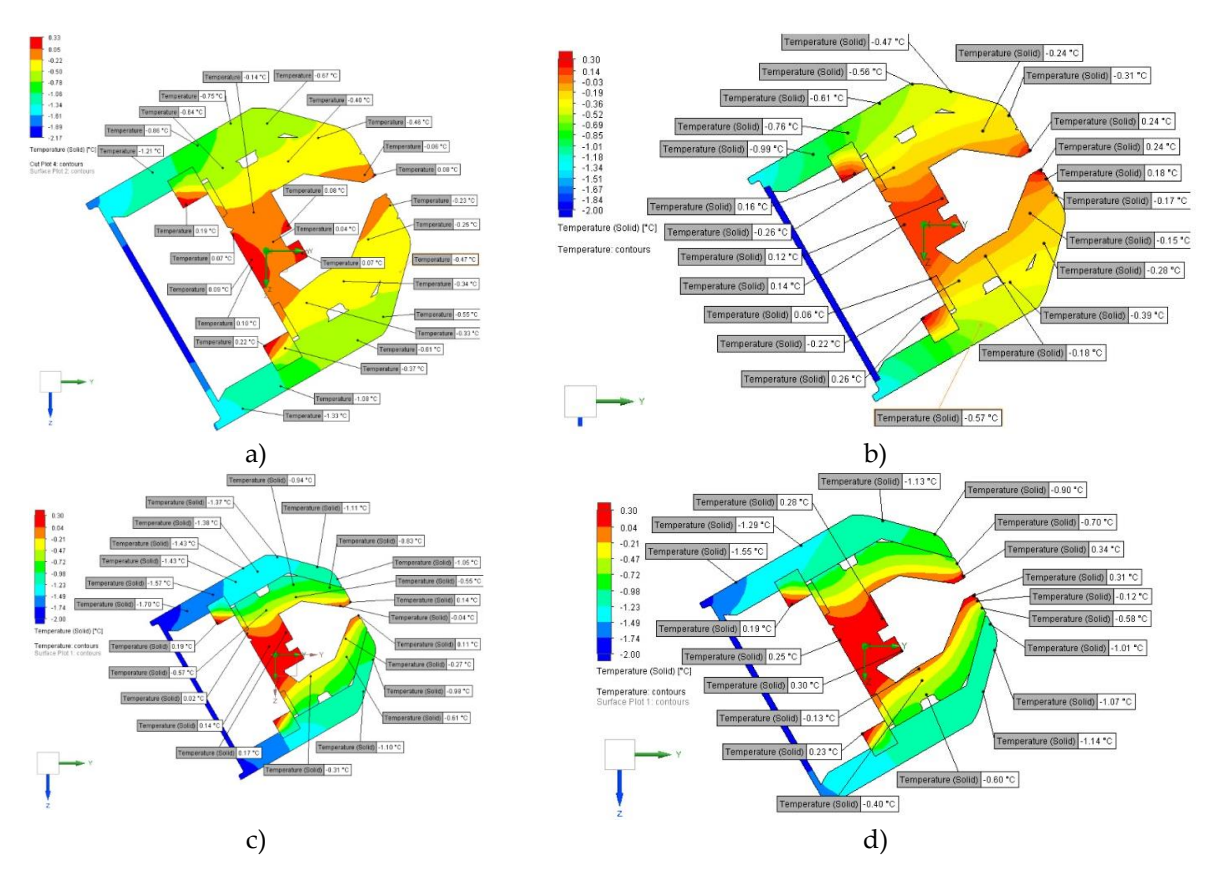


**Fig. 17.** Temperature distribution of solid elements - YZ cross-section view of the nozzle: a) p = 15 bar, swirler and atomizer material: MO58; b) p = 40 bar, swirler and atomizer material: MO58; c) swirler and atomizer material:  $Al_2O_3 - 98\%$ ; d) p = 40 bar, swirler and atomizer material:  $Al_2O_3 - 98\%$ 

### 5. Conclusions

Considering the fundamental importance of optimizing water nozzles in snowmakers, based on numerical modeling performed using Simcenter FLOEFD for NX, it can be concluded that:

- the temperature distribution maps presented on the nozzle outlet surface indicate that the nozzle will not freeze within the outlet for the specified boundary conditions;
- the nozzle design allows for free water flow within it. To optimize flow parameters, it is recommended to introduce a fillet radius at the transition from cylinder to cone geometry in the nozzle element.

Both the swirler and atomizer materials, MO58 brass and Al<sub>2</sub>O<sub>3</sub> 98% aluminum oxide, for pressures of 15 bar and 40 bar, can be successfully used in industrial environments. The choice of a specific solution will depend not only on atmospheric conditions but should also take into account the criteria of material wear, replacement, availability, and economic competitiveness.

The article was prepared as part of project no.: POIR.01.01.01-00-0522/19-00

#### References

[1] Kalukiewicz A.: Mining Applications of High-Pressure Water Jets – Theory, Research, and Industrial Applications. AGH Publishing House, Kraków, 1997. (In Polish).

- [2] Prostański D.: Air-water spraying method for reducing the methane and coal dust explosion hazard as well as for reducing the airborne dust concentration. Scientific Works Monographs No. 51. KOMAG Institute of Mining Technology, Gliwice, 2017. (In Polish).
- [3] Orzechowski Z., Prywer J.: Production and application of sprayed liquids. PWN S.A. Scientific Publishers, Warsaw, 2018. (In Polish).
- [4] Li J. W., Liu Y., Qin L. Z.: Numerical Simulation of Flow and Heat Transfer in Round-to-Rectangular Nozzles. *Numerical Heat Transfer, Part A: Applications*. 2007, *51*(3), 267–291.
- [5] Reis L.B., dos Santos Gioria R.: Optimization of liquid jet ejector geometry and its impact on flow fields. Applied Thermal Engineering. 2021, 194. Doi: 10.1016/j.applthermaleng.2021. 117132
- [6] Kuś T., Madejski P.: Numerical investigation of thermal-flow processes in the ejector-condenser for selected geometrical parameters. *Archives of Thermodynamics*. 2024, vol. 45 no. 4, s. 73–83.
- [7] Buska D., Madejski P., Karch M.: Rapid prototyping of water nozzles using CFD modeling and 3D printing results. *Mining Informatics, Automation and Electrical Engineering*. 2023, R. 61, nr 3, 7—21.
- [8] Wen J., Chen C.: Optimizing the Structure of the Straight Cone Nozzle and the Parameters of Borehole Hydraulic Mining for Huadian Oil Shale Based on Experimental Research. *Energies*. 2017, 10, 2021.
- [9] Jiang T., Huang Z., Li J., Zhou Y., Xiong C.: Effect of Nozzle Geometry on the Flow Dynamics and Resistance Inside and Outside the Cone-Straight Nozzle. *ACS Omega*. 2022, Vol 7/Issue 11, 9652–9665.
- [10] Pan Y., Geng Z., Yuan H., Zhai S., Huo F.: Numerical Simulation and Flow Field Analysis of Porous Water Jet Nozzle Based on Fluent. *Appl. Sci.* 2024, *14*, 7075.
- [11] Ballesteros Martínez M., Gaukel V.: Time-Averaged Analysis and Numerical Modelling of the Behavior of the Multiphase Flow and Liquid Lamella Thickness Inside an Internal-Mixing ACLR Nozzle. *Flow Turbulence Combust.* 2023, 110, 601–628.
- [12] Barth T., Ohlberger M.: Finite volume methods: Foundation and analysis. Encyclopedia of Computational Mechanics. Edited by Erwin Stein, Rene de Borst and Thomas J. R. Hughes, John Wiley & Sons, Ltd. 2004.
- [13] Laurence D., Uribe J.: The Finite Volume Method. Code\_Saturne training, School of Mechanical, Aerospace and Civil Engineering, Manchester United Kingdom 4-6 July 2011.
- [14] Polish Standard PN-EN 12164:2016. Copper and copper alloys Rods for machining. (In Polish)
- [15] Polish Standard. PN-M-73093\_11x1. Circular cross-section seals. O-rings.
- [16] Supers now, https://www.supersnow.pl/ (accessed on 20 October, 2025)

